Satellite based wind resource assessment over the South China Sea

Badger, Merete; Astrup, Poul; Hasager, Charlotte Bay; Chang, Rui; Zhu, Rong

Published in:
Proceedings of China Wind Power conference (CWP 2014)

Publication date:
2014

Document Version
Peer reviewed version

China Wind Power 2014

Category: Wind resource assessment

Satellite based wind resource assessment over the South China Sea

Merete Badger[1], Poul Astrup[1], Charlotte Bay Hasager[1], Chang Rui[2], Zhu Rong[3]

1. Technical University of Denmark, Department of Wind Energy, Roskilde, Denmark

2. Public Meteorological Service Center of CMA, Beijing, 10081

3. National Climate Center, Beijing, 10081

Abstract

Wind maps from satellites cover large areas and show horizontal wind speed variations offshore in great detail. This information is an excellent supplement to mast observations, which are limited to specific points, and to model simulations, which are typically run at coarser resolution. Wind maps from satellite synthetic aperture radar (SAR) data are particularly suitable for offshore wind energy applications because they offer a spatial resolution up to 500 m and include coastal seas. In this presentation, satellite wind maps are used in combination with mast observations and numerical modeling to develop procedures and best practices for satellite based wind resource assessment offshore.

All existing satellite images from the Envisat Advanced SAR sensor by the European Space Agency (2002-12) have been collected over a domain in the South China Sea. Wind speed is first retrieved from the raw satellite observations of radar backscatter from the sea surface. The backscatter is closely related to the surface wind stress and the instant wind speed. An empirical model function is applied, which describes the backscatter-to-wind relationship for the standard height 10 m above the sea surface. The satellite winds are compared against observations from a network of coastal meteorological masts.

A statistical analysis is performed to estimate the wind resources. The outcome is a series of maps showing the mean wind speed, Weibull parameters, wind power density, and uncertainties. Wind variations are clearly visible across the domain; for instance sheltering effects caused by the land masses. The satellite based wind resource maps have two shortcomings. One is the lack of information at the higher vertical levels where wind turbines operate. The other is the limited number of overlapping satellite samples which can be collected due to the satellite orbit dynamics. Both challenges are addressed.

A novel methodology is applied to project the satellite wind resource maps from 10 m to higher vertical levels by means of simulations from the Weather Research and Forecasting (WRF) model. Three years of WRF data – specifically the parameters heat flux, air temperature, and friction velocity – are used to calculate a long-term correction for atmospheric stability effects. The stability correction is applied to the

satellite based wind resource maps together with a vertical wind profile description in order to calculate the mean wind climate at different levels up to 100 m.

Time series from coarser-resolution satellite wind products i.e. the Special Sensor Microwave Imager (SSM/I) data are used to calculate the long-term temporal variability of the wind climate. This can be used to compensate for the limited number of satellite SAR samples. Altogether, the study demonstrates how a combination of several data types adds to the accuracy and the representativeness of wind resource assessment offshore.

Introduction

The project 'Study on offshore wind resource assessment based on satellite data and modeling' (ORES), is a 2-year (2013-14) collaborative effort between the Wind Energy Department of the Technical University of Denmark (DTU Wind Energy) and the Public Meteorological Service Center of China Meteorological Administration (PMSC/CMA) in China. The project objective is to develop a validated methodology for offshore wind resource assessment in China based on satellite data and numerical modeling.

Study area and data

The project focuses on a study area in the South China Sea. The area covers the coastline of the Guandong province and includes also the island of Hainan Dao. Several types of satellite data have been collected over the study area and the WRF mesoscale model has been run. In addition, the project team has access to a large amount of coastal and offshore meteorological stations distributed over the area. Figure 1 shows a map of the study area with indication of three meteorological stations, which are used in this paper.

Figure 1. Map of the study area with indication of three meteorological masts. Image courtesy: Google Earth.

Winds from satellites

Four types of satellite data with different image properties have been collected over the South China Sea. The main differences between the products from the user's perspective lie in their spatial resolution and their spatial and temporal coverage. All of the satellite wind products give wind information at 10 m above the sea surface.

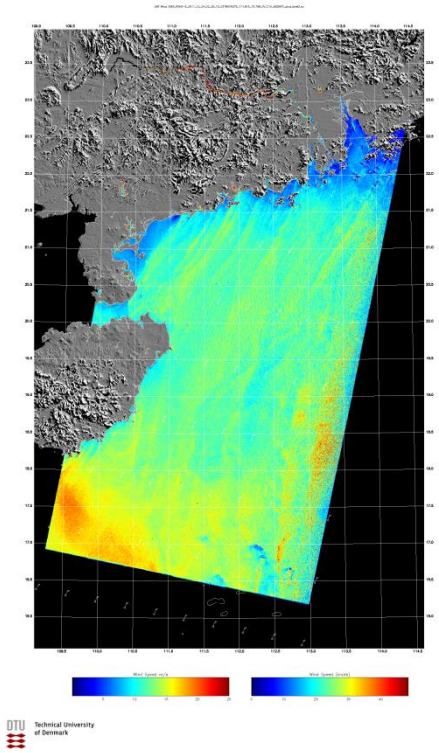

Figure 2. Wind speed map retrieved from Envisat ASAR for December 24, 2011 at 02:36 UTC. Wind barbs show the wind speed and direction from the NOGAPS model.

High-resolution satellite data are obtained from the Envisat Advanced Synthetic Aperture Radar (ASAR) by the European Space Agency. The data are acquired in Wide Swath mode (WSM) with a spatial resolution of 150 m for the raw SAR data. Resampling to 500 m is performed to eliminate effects of random noise in the data. The SAR provides observations of radar backscatter from the sea surface, which are related to the sea surface roughness within the same spectral range as the SAR pulses (i.e. cm-scale waves). Wind retrieval from SAR observations of radar backscatter is typically performed by the data users. In this study the processing of wind speed maps is performed with the Geophysical Model Function (GMF) called CMOD5.n [1]. The GMF defines the empirical relationship between the instant wind speed and the radar backscatter in C-band with vertical polarization. Some of the SAR scenes are acquired with horizontal polarization. The polarization ratio model 1 by Mouche et al. [2] is applied to correct for this. Wind directions from the US Navy Operational Global Atmospheric Prediction System (NOGAPS) are used in order to calculate the wind speed (only one of these two parameters can be retrieved from SAR). Figure 2 shows an example of a SAR wind speed map.

Coarser-resolution satellite data are obtained from two scatterometers: QuikSCAT which operated during the years 1999-2009 and ASCAT, which has been in operation from 2007 to present. The principle of operation is similar for SAR and scatterometry except that scatterometers scan each observed area from multiple angles whereas SAR only observes from one angle. This facilitates simultaneous wind speed and direction retrieval from scatterometers. The backscatter-to-wind processing is usually performed by the data providing agencies and wind data is readily available for download. The grid cell size of the data used here is 25 km for QuickScat and 12.5 km for ASCAT.

The Special Sensor Microwave/Imager (SSM/I) is a series of satellite sensors which have delivered data since 1987. The data is retrieved from passive microwave radiometer observations of the sea surface and the principle operation is thus different from the active microwave sensors described above. SSM/I instruments provide wind speed only and the wind speed is derived from observations of the brightness temperature of the sea surface, which again depends on the surface roughness [3]. The SSM/I data is gridded to 0.25° and readily available for download from Remote Sensing Systems. In this study, a time series from 1988-2013 is used.

Numerical modeling

The Weather Research and Forecasting model (WRF) has been run for the three years 2009-11 to simulate the wind climate over the study area at 5 km and 15 km spatial resolution for domain 2 and domain 1. We have used version 3.4 of the Advanced Research WRF (ARW-WRF) and the model setup is identical to the one used by Hahmann et al. [4].

Mast observations

The project has access to a network of meteorological stations provided by the Climate Center of Hainan Meteorological Bureau. The on-site observations make it possible to perform step-by-step comparison of the methodology under development. Each meteorological mast provides hourly mean values of wind speed and direction observations at the height 10 m. Three masts called 59765, M1175, and M1328 are utilized in this study and their locations are indicated in Figure 1. Table 1 shows the period of operation for each mast.

Table 1. Periods of operation for the three meteorological masts used in this study.

Met mast	Period
59765	20100723-20121231
M1328	20100504-20121231
M1175	20090101-20121012

Validation of satellite data

The 10-m satellite winds are compared against the mast observations. Due to the different periods of operation, the number of co-located mast and satellite samples is limited. This problem is particularly pronounced for the SAR data set because SAR data acquisitions are irregular and limited to 100 scenes or less per year over the study area. Results of the comparison of SAR and in situ wind speeds are shown in Figure 3. The correlation coefficient (R) is within the range 0.7-0.8 for the three stations investigated whereas the standard deviation (STD) is 2.0-2.5. For the mast M1175, the point cloud does not follow a 1:1 trend line. This might be a consequence of the proximity of this station to the land. Separation of the samples into onshore and offshore wind directional sectors leads to a significant improvement of the statistical results for this station when there is a large fetch (R=0.8, STD= 2.5). For the other two stations, which are located on islands in the open sea, the data points are distributed more evenly around the 1:1 line.

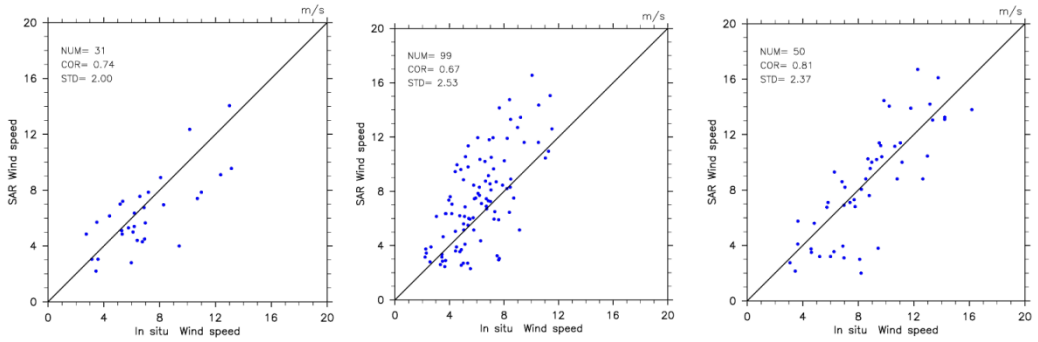

Figure 3. In situ wind speeds from 59765 (left), M1175 (middle), and M1328 (right) versus SAR wind speeds. NUM indicates the number of co-located samples, COR is the correlation coefficient (R), and STD is the standard deviation.

Table 2 summarizes the results of comparisons for the scatterometer wind speed and direction. The correlation on wind directions is consistently close to 0.9 which is very satisfactory. For the wind speed comparisons, the correlation is again poor at station M1175 but close to 0.8 for the two other masts compared to ASCAT. These stations were not yet in operation when the QuikScat data were acquired. It is important to note that the satellites provide the equivalent neutral wind (ENW) whereas the masts give the real wind. This might explain some of the deviation between satellite and in situ winds shown here.

Table 2. Overview of validation results for QuikScat and ASCAT wind speed and directions.

		Wind direction			Wind speed		
Satellite sensor	Mast	N	R	STD	N	R	STD
QuikScat	M1175	35	0.89	33.6	37	0.59	2.2
ASCAT	M1328	55	0.88	27.6	64	0.82	2.2
	59765	352	0.87	30.9	366	0.79	1.8

Satellite based wind resource maps

Wind resources at the 10-m level are calculated through fitting of a Weibull function to all the available satellite SAR and scatterometer wind data. The procedure is repeated for every point in a regular grid over the study area as described in previous works [4,5]. The outcome is a series of maps showing the mean wind speed, the Weibull scale and shape parameters, the wind power density, and sampling uncertainties. Figure 4 shows the number of overlapping SAR scenes that could be achieved for the study area and the mean wind speed generated from the SAR data over the study area. Striping in the wind speed map results from the variable number of SAR samples.

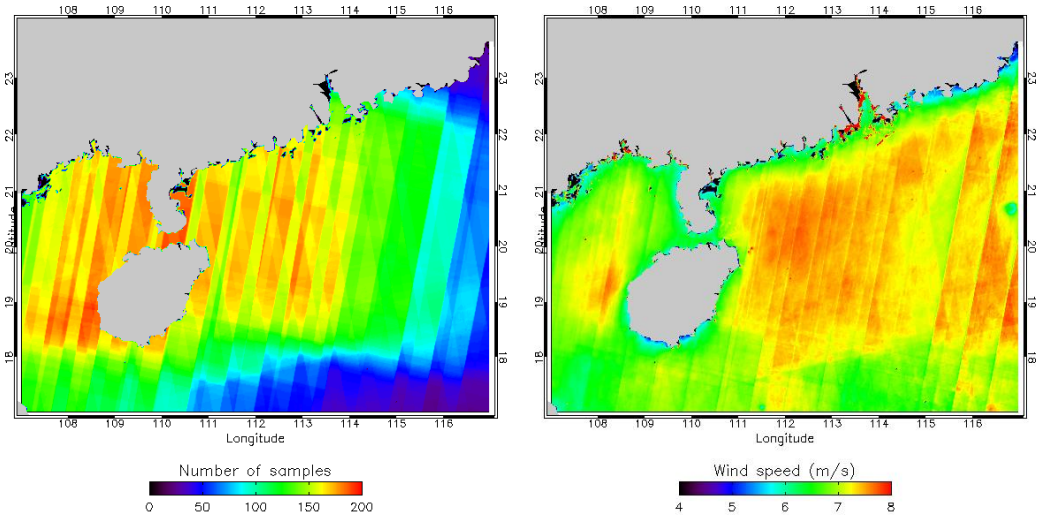

Figure 4. Maps showing (left) the number of overlapping satellite scenes and (right) the 10-m mean wind speed from all available SAR scenes over the study area in the South China Sea.

Vertical wind variability

The mean wind conditions calculated from each of the different satellite data types are used in combination with a vertical wind profile description to calculate the mean wind speed at different levels up to 100 m. The vertical wind profile is established from Equation 1:

$$\left\langle \frac{\kappa\, u(z)}{u_*} \right\rangle = \ln\left(\frac{z}{z_0}\right) - \langle \psi_m \rangle \qquad (1)$$

where u is the wind speed at a given height, z, and u_* is the sea surface friction velocity. z_0 is the aerodynamic roughness length and κ is von Karman's constant. The parameter ψ_m is a long-term stability correction, which can be calculated from Monin Obukhov similarity theory as described by Peña and Hahmann [7]. In this analysis, the correction for atmospheric stability is calculated from output parameters of the WRF simulations – specifically the heat flux (*HFX*), air temperature (*T2*), and friction velocity (*UST*). Figure 5 shows the long-term stability correction and the resulting vertical wind profile for a point in the South China Sea.

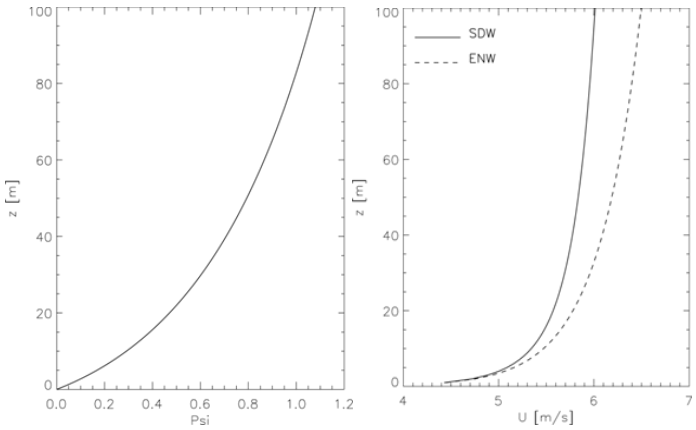

Figure 5. Plots showing the vertical distribution of (left) the long-term stability correction and (right) the mean wind speed calculated with (SDW) and without (ENW) stability correction.

The stability correction is positive all over the study area in the South China Sea indicating that the atmospheric conditions are unstable at all times. This is due to the very warm sea water in the area. As a consequence, winds at 100 m decrease by 0.5 m/s when the correction for atmospheric stability is applied. It is thus very important to take stability into account for this area.

Long-term wind variability

Based on the SSM/I data set, the long-term variation (1988-2014) of the 100-m mean wind speed has been calculated for every month of the year at specific points in the study area. Figure 6 shows an example from Guandong East. The mean wind speed is much higher during the winter months (October-February) than for the rest of the year. The long-term trend shows increasing mean wind speeds for some months and decreasing for others. The reason for these trends is unknown.

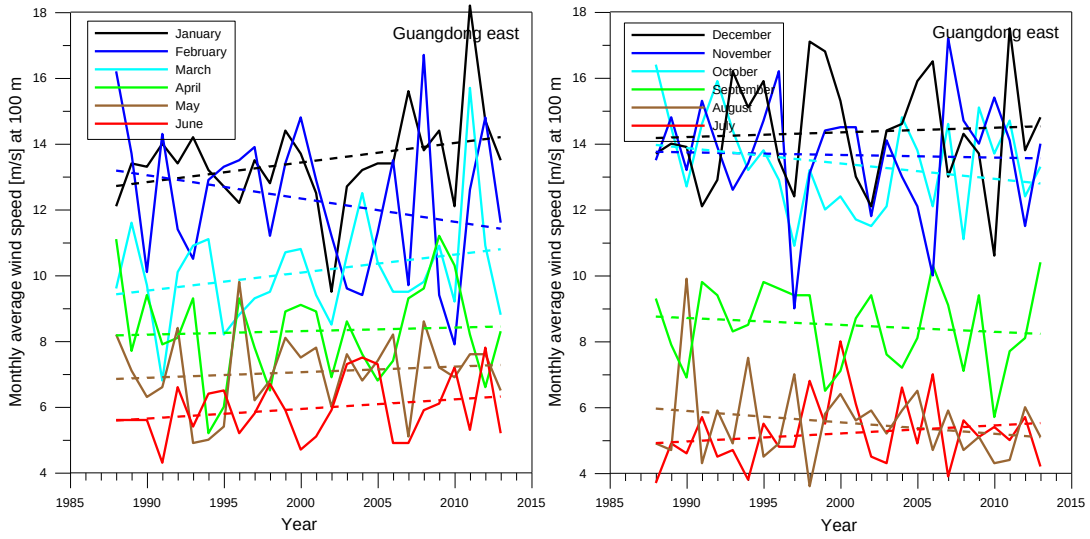

Figure 6. Plots showing trends of the mean wind speed from SSM/I data for a point in the South China Sea during the period 1988-2013 and for each calendar month (left: January-June and right: July-December).

Conclusions and future work

This analysis has demonstrated how different types of satellite data, numerical modeling, and on-site wind observations can be used synergistically for wind resource assessment offshore. Comparison of the satellite winds against co-located mast observations show a satisfactory level of accuracy which was similar for SAR and scatterometer winds. The satellite winds can thus be used with confidence over the South China Sea. The combination of satellite data and numerical modeling described here helps to overcome the two most important shortcomings of satellite observations: 1) the lack of information at vertical levels beyond 10 m, and 2) the limited number of overlapping satellite samples which can be collected. A further integration of satellite observations and WRF model simulations can be achieved through assimilation of the satellite data into the WRF modelling chain. Another way to integrate the data sets further is to make a direct coupling between SAR and scatterometer observations of instant winds with the long-term wind variability given by SSMI/I data and WRF model simulations over several decades.

Acknowledgements

The project 'Study on offshore wind resource assessment based on satellite data and modeling' (ORES) is funded by the Sino-Danish Renewable Energy Development Programme (RED). Meteorological mast observations are provided by the Climate Center of Hainan Meteorological Bureau. Satellite SAR data are from the European Space Agency, QuikSCAT data are provided by the Asia-Pacific Data-Research Center (APDRC), ASCAT data are from the US National Oceanic and Atmospheric Administration (NOAA). SSM/I and SSMIS data are produced by Remote Sensing Systems and sponsored by the NASA Earth Science MEaSUREs Program and are available at www.remss.com.

References

[1] H. Hersbach, "Comparison of C-Band Scatterometer CMOD5.N Equivalent Neutral Winds with ECMWF," *J. Atmos. Ocean. Technol.*, vol. 27, no. 4, pp. 721–736, 2010.

[2] A. A. Mouche, D. Hauser, J. F. Daloze, and C. Guerin, "Dual-polarization measurements at C-band over the ocean: Results from airborne radar observations and comparison with ENVISAT ASAR data," *IEEE Trans. Geosci. Remote Sens.*, vol. 43, no. 4, pp. 753–769, 2005.

[3] F. J. Wentz, "SSM/I Version-7 Calibration Report,". RSS Technical Report 011012, Santa Rosa, 46p., 2013. Available at: http://images.remss.com/papers/rsstech/2012_011012_Wentz_Version-7_SSMI_Calibration.pdf

[4] A. N. Hahmann, J. Lange, A. Peña, and C.B. Hasager, "The NORSEWInD numerical wind atlas for the South Baltic," DTU Wind Energy, 53 p., 2012 (DTU Wind Energy E; No. 0011(EN))..

[5] C. B. Hasager, M. Badger, A. Pena Diaz, X. G. Larsén, and F. Bingöl, "SAR-based Wind Resource Statistics in the Baltic Sea," *Remote Sens.*, vol. 3, no. 1, pp. 117–144, 2011.

[6] R. Chang, R. Zhu, M. Badger, C. Hasager, R. Zhou, D. Ye, and X. Zhang, "Applicability of Synthetic Aperture Radar Wind Retrievals on Offshore Wind Resources Assessment in Hangzhou Bay, China," *Energies*, vol. 7, no. 5, pp. 3339–3354, 2014.

[7] A. Peña and A. Hahmann, "Atmospheric stability and turbulence fluxes at Horns Rev—an intercomparison of sonic, bulk and WRF model data," *Wind Energy*, vol 15, no. 5, pp. 717-731., 2012. DOI 10.1002/we.500.